

Stroke Trajectory Generation Experiment for a Robotic Chinese Calligrapher Using a Geometric Brush Footprint Model

Josh H. M. Lam and Yeung Yam, Senior Member, IEEE

Abstract—This paper describes a method to generate stroke trajectories executed by a 5-DOF robotic art system. A brush footprint model is proposed to represent the footprint outline, which is sensitive to the applied stress. After extracting real brush footprints from experiments, the model parameters are obtained using linear regression. Trajectories are searched along the segmented strokes of Chinese characters by varying the shape of brush footprint. The generated trajectory is 5-DOF, which is compatible to the robot art system. Simulations and experiments were conducted using calligraphy of Bada Shanren, a famous Chinese ancient artist, as an example.

I. INTRODUCTION

Creating robots with human characteristics has been a ultimate intention for many research groups. They have developed robots to emulate human motions and other personalities [1]-[3]. Art is a performance that only human being is capable to carry out. This unique activity provides a manner for spiritual expressions in form of paintings and other artworks. Many artistic robots have been investigated to emulate this human behavior in the last century [4]-[8]. They act as an augmentation to help people creating artworks.

Chinese calligraphy is a significant art in Chinese culture that a brush is manipulated to write Chinese characters. The formation of the calligraphy is determined by the locus of brush footprint. Typical brush footprint models are used as a virtual brush ([9]-[14]). It works with input devices to capture human hand motions and generates brush strokes. The brush footprint model in [9] proposed that the cross-section of a brush can be viewed as an ellipse. To vary the width of a stroke, the applied pressure is changed to affect its cross-section. Hence, when an artist draws with a brush, the strokes are combinations of the elliptic imprints. In fact, a brush footprint cannot be represented in this way in real situations, basically because of the mismatch of footprint geometry. Also, the corresponding aspect ratio does not apply real information, so they cannot predict the shape variation of actual brush footprints.

To use real brush footprint information for a 3-DOF configuration, our group has introduced a representation of brush footprints by database of brush footprint images [14]. A special setup is used to visualize the brush footprints. A brush moves in a transparent container, which contains colored solution. When it is contacting the container with different pressure levels, a camera beneath captures the shape of the

varying brush footprint. As both events are synchronized, the system would accurately capture the change of footprint caused by the brush deformation on glass plane. The collection of images is adopted as a database, and would cooperate with a genetic algorithm based trajectory searching method. However, the brush footprint images acquisition method requires colored water as media to visualize the brush footprints. The environmental condition would be different from actual writing situation, so uncertainties would exist and cause the brush deforms differently. Hence, to obtain the accurate results, we should draw the brush footprints on paper for capturing.

In this paper, a 5-DOF stroke trajectory generation method for Chinese calligraphy is presented. It works with a brush footprint model constructed based on information acquired from experiments. It is converted to a proposed representation using linear regression. The trajectory searching process is superimposing brush footprints on segmented strokes of a Chinese character, such that strokes are covered. If the trajectory is found to cause outlying regions, it would be modified to alleviate such problem.

II. INTELLIGENT ROBOTIC ART SYSTEM

An art robot called Intelligent Robotic Art System (IRAS) has been developed recently by our research group for replication and rendering of artworks. The configuration of IRAS is shown in Figure 1(a) that it is a drawing platform, which contains a 5-DOF manipulator. It can move in x, y and z translational directions to execute trajectories for plane drawing. Two additional rotation joints in roll and pitch enable the robot to control painting brush or even Chinese writing brush with dexterous motions. A clip is located at the terminal of manipulator and so that different types of drawing tools, such as pencil, paint brush, or even Chinese writing brush, can be mounted onto the manipulator for different drawing styles. To enhance the output line smoothness, a PID controller is used in the system positioning to minimize the superfluous oscillation during operation. Moreover, a camera is also mounted at the side of the platform to capture the drawing procedure and outcomes. The captured images can be re-projected to top view by homography.

An additional axial rotary brush is also installed on the manipulator. A photo of the brush is shown in Figure 1(b). The rotary brush contains a servomotor and a brush holder part, which locks a brush along the axis of the motor. So, once the servomotor actuated, it rotates the brush holder as well as the brush. The servomotor cannot improve the workspace of

Manuscript received March 1, 2009. Josh H.M. Lam and Yeung Yam are with the department of Mechanical and Automation Engineering in the Chinese University of Hong Kong, HKSAR, China. (e-mail: hmlam, yyam@mae.cuhk.edu.hk)

the robot, as its axis is coaxial to that of the brush. But, it enables different sides of a brush contact with the horizontal surface. This rotational motion is essential for hairy brush, since artists rotate a brush to ink and straighten the brush hair. With the planned motion, the robot is capable to ink and absorb the excessive ink in a brush. When the hair is deformed, it can also be used to straighten the brush hair automatically.

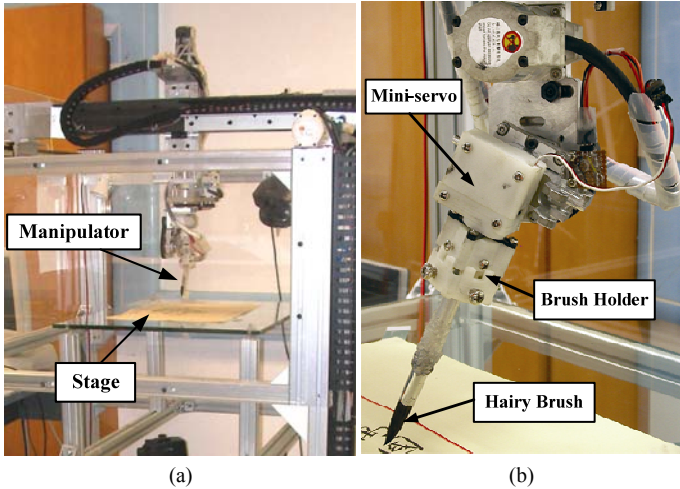


Figure 1. Photos of (a) IRAS and (a) its axial-rotary brush.

III. MODEL ACQUISITION OF BRUSH FOOTPRINT

A. Brush Footprint Representation

Brush footprint can be considered as the projection of a brush onto the contacting surface. It is normally a water-droplet-like shape with a sharp tip as indicated in Figure 2,

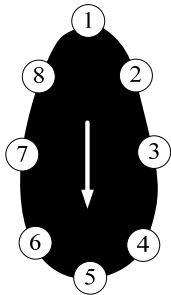


Figure 2. Indication of point sequences for boundary sampling and the longitudinal direction

and symmetric about a vertical center line. Our acquisition method for brush footprint is in principle to obtain its approximated shape. Hence, the shape boundary can be represented by a geometric shape with several vertices, which are indicated by the write circles in the figure. A brush footprint is sampled clockwise along its boundary starting from the brush tip (vertex 1). When we are writing Chinese calligraphy, the brush footprint is

deformed mainly by the reaction force of the contacting surface. We assume this reaction force is affected by the varying applied pressure level (or the height of brush insertion) and brush inclination. Therefore, the measurement for acquisition of brush footprint involves both factors.

B. Experimental Acquisition of Brush Footprint

Normally, if a stroke is written using a brush, the previous brush footprints would be overlapped by the current one. However, we discovered that the intensity of the color in the brush footprint is affected by the amount of condensed ink. In

addition to this, the excessive ink in a brush should be well absorbed before writing. Otherwise, ink diffusion would significantly distort the brush footprint.

Consider that a brush is kept vertical and pressed on a surface by a vertical motion, the brush hair would be bent. So brush footprints are deformed to be irregular shapes, until the brush moves horizontally to straighten them. Therefore, the motion of the manipulator should be constrained to prevent this occurs. The direction of motion, called longitudinal direction, is indicated by the white arrow in Figure 2. Figure 3 shows the procedures to ensure the brush keeping straightened. The brush is first moved on the paper and adjusted to the required inclination, such that the brush tip is touching the on it (Figure 3(a)). Then, the manipulator moves in the longitudinal direction and presses it down to increase the pressure as shown in Figure 3(b). The brush further moves in this direction until it reaches to both the desired position and applied brush pressure level (Figure 3(c)).

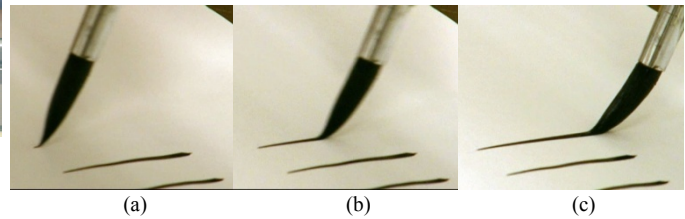


Figure 3(a)-(c). Images of brush motion to draw a stroke

The brush is stopped at the position for several seconds after drawing a stroke. This condenses extra ink on the brush footprint, which color would be deepened. So the footprint can be visualized. From the stroke in Figure 4(b), a footprint is displayed with darker color compared to the stroke part, so the boundary can be apparently observed. The robot continues to draw strokes with different inclinations and applied pressure levels. In our experiment, the brush inclination was exampled from 5° to 50° every 5° , while the pressure level was from 1 mm to 15 mm every 1 mm. Each stroke is 50 mm length and is separated by a 20 mm interval as shown in Figure 4(a). To mark the actual positions of the brush footprints, a reference line is drawn aside and perpendicular to the stroke direction.

After drawing all the strokes, they are input as digital image for further image processing. Most of the brush footprints can be extracted automatically by thresholding, as the color tone of the brush footprints is slightly different from that of the stroke. Then top and bottom sample points (1 and 5) are first chosen, which distance is the length of a brush footprint. However, the contrast in the strokes may be influenced by the light intensity in image conversion process, which obscures this difference. So, in that case, we should manually adjust these two sample points.

Then, two perpendicular lines are drawn as reference, and are indicated by red dot lines in Figure 4(c). The horizontal line is the one for position marking. As we assume the brush footprint is a symmetrical shape, the vertical line is its center line. However, there would be uncertainties in the experiment,

which makes the top and bottom sample points cannot lie on the same vertical line. To reduce this error, a vertical line with minimized horizontal distance is selected. Afterwards, three horizontal lines (the blue lines in Figure 4(c)) are generated to split the center line into 4 portions. At the same time, each of them intersects the boundary of the brush footprint in each symmetric half. All these points are recognized to be the sample points (2-4 and 6-8 in Figure 2), which locate at both sides of a brush footprint. We also observe that a brush footprint has the largest wide in its middle part, which is the distance between sample points 3 and 7. So, the distance is called wide of a brush footprint, and the center is the mid point of these two sample points.

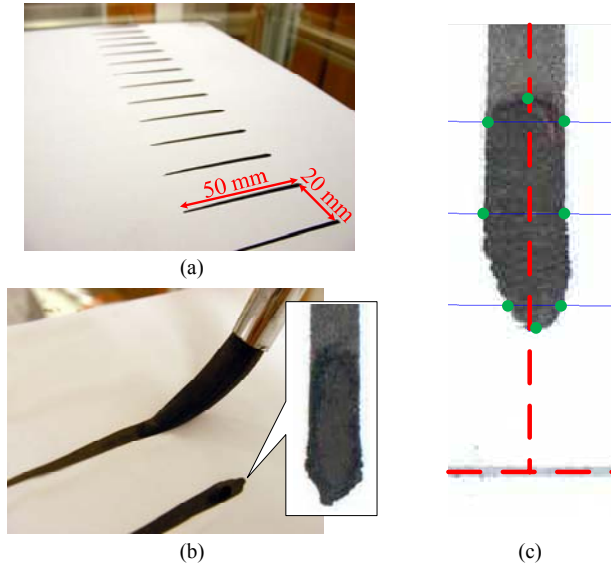


Figure 4. (a) strokes drawn by IRAS, (b) a stroke with a residual shape and (c) boundary sampling of the brush footprint.

The captured brush footprints were converted into the proposed model as polygons with 8 vertices. For a real brush footprint, it shows a trend of shape changes. The brush footprint would be enlarged, once higher brush pressure is applied or the brush vertical inclination increases. In our point acquisition of brush footprints, all the vertices of the model retain the same tendency of changes. Figure 5 shows some of the brush footprints in the model. Each brush footprint is illustrated with different colors to indicate each individual. Figure 5(a) shows the model varies in pressure level with constant brush vertical inclinations. It can be observed that the sizes of the footprints are expanded, when the brush pressure is increased. For the footprint shown in Figure 5(b), it reveals the relation between the shapes of footprints to the brush vertical inclination. It is found that the brush footprint is enlarged, similar to that with increasing applied brush pressure. The center of it is also shifted simultaneously in the brush tip direction. In this observation, the model shows a tendency of variations to changing brush position and orientation in continuous motions.

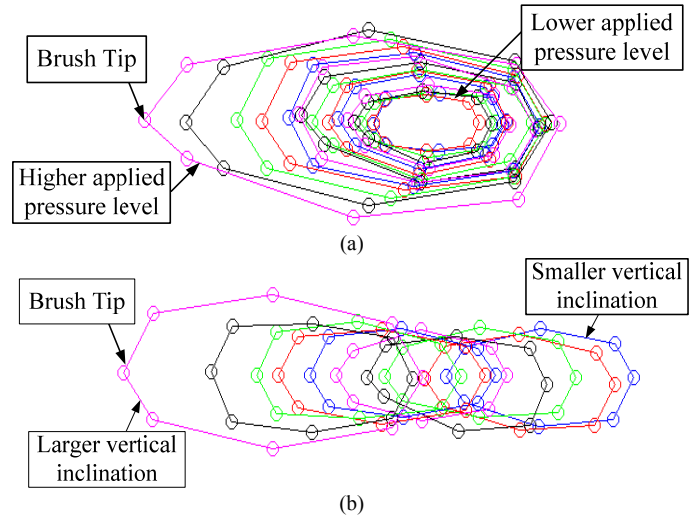


Figure 5. Illustration shows the relations of acquired brush footprints to (a) applied pressure levels and (b) brush inclinations

C. Model Formation Using Linear Regression

In the proposed model, each brush footprint is represented by a geometric shape with 8 vertices. The previous section demonstrated a tendency of change exists in the vertices, if the positioning parameters varied. In essence, our model approximates and predicts this change. If the acquired geometric shapes are directly used, they cannot entirely describe a motion with their discrete property. In other words, these changes should be interpolated as continuous descriptions. Hence, the changes in vertices can be efficiently represented using 16 polynomials (x and y coordinates of all the 8 vertices).

Consider that the polynomials $f(d, \gamma)$ for the coordinates can be expressed in form of

$$f(d, \gamma) = \sum_{i=0}^m \sum_{j=0}^n a_{ij} d^i \gamma^j \quad (1)$$

where a_{ij} is coefficient in the function, d is the applied pressure level, γ is the vertical brush inclination, m and n denote the power orders of d and γ respectively. Therefore, a_{ij} and $d^i \gamma^j$ are linearly involve in $f(d, \gamma)$. By rewriting the function,

$$y(d, \gamma) = A^T \phi \quad (2)$$

where $y(d, \gamma)$ is the measurement of the corresponding coordinate in one of the vertices $A = [a_{11} \ a_{12} \ \dots \ a_{mn}]^T$ and $\phi = [d\gamma \ d\gamma^2 \ \dots \ d^m \gamma^n]^T$. If we assume the uncertainty of measurement is least square type, the problem can be solved using linear regression to obtain A . Recall the solution of the regression,

$$A = (X^T X)^{-1} X^T Y \quad (3)$$

where $X = [\phi_1 \ \phi_2 \ \dots \ \phi_m]^T$, $Y = [y_1 \ y_2 \ \dots \ y_m]^T$ and m is the number of measurements for the same coordinate. According to Figure 5, both figures show that each vertex is varied with constant tendency. So, even low order

polynomials would be effective to give an interpolation with small error. Here, we have chosen $m=3$ and $n=3$ in (1). Result shows that the interpolated vertices with negligible errors to the measurements. A mesh represents the distance between a vertex and the center of brush footprint is shown in Figure 6. The mesh is apparently smooth, which infers the global optimal solution can be obtained simply in the trajectory searching process.

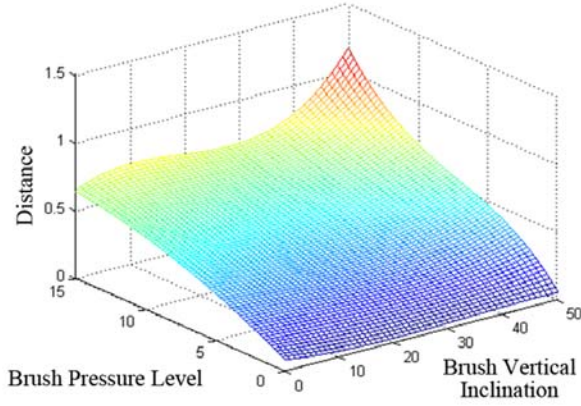


Figure 6. A mesh shows the distance of a sample point to the center of brush footprint

IV. STROKE TRAJECTORY GENERATION FOR ROBOTIC CHINESE CALLIGRAPHY

The fundamental idea of calligraphic trajectory generation is to superimpose brush footprints to fully cover the strokes in a Chinese character. Our group has proposed a method based on genetic algorithm (GA) in [14] and [15] to create 3-DOF stroke trajectories. It maps brush footprints along the medial axes of strokes. The sizes of the footprints are changed, depends on the random strategy in GA, both the outside area of footprints and uncovered regions are minimized. However, for 5-DOF trajectory searching, the problem would be more complicated with 2 additional DOFs. Hence, GA may not guarantee the searching reaches optimum in limited time. Therefore, certain criteria should be formulated to make the problem compatible to other optimization approaches.

A. Searching with Identical Stroke Width

After stroke segmentation of a Chinese character using the approach in [16], the strokes are represented in form of medial axes and cross-section lines. To simplify the searching problem, some conditions should be fulfilled to limit the searching range of trajectory parameters. In the acquisition process of brush footprints, the manipulator was executed to move the brush in the longitudinal direction to induce residual brush footprints. For this reason, the searching should also follow this direction, which is the gradient of a point on a stroke medial axis. Otherwise, it would change the friction between the brush and the paper. The brush footprint would be deformed differently compared to the one moving in longitudinal direction. Therefore, to reduce the possibility of variation, the direction of movement is limited, which is an important criterion, in this 5-DOF trajectory searching.

Moreover, the shape of brush footprint is almost symmetrical along its longitudinal axis. As mentioned, it has the largest width in the middle part, which is close to the distance between point 3 and point 7. Conceptually, if the brush can write strokes with identical stroke widths, it would generate same strokes. As cross-section lines are output from the stroke segmentation, which can be considered as the stroke widths. So, the center of brush footprint is supposed to touch the medial axis. The problem can be formulated as minimizing the difference of stroke width and the width of brush footprint, which can be expressed as:

$$\begin{aligned} & \text{minimize } x_3(d, \gamma) - x_7(d, \gamma) - W_s \quad (4) \\ & \text{subject to } d, \gamma > 0 \end{aligned}$$

where $x_3(d, \gamma)$ and $x_7(d, \gamma)$ are the x coordinates of sample points 3 and 7 of the brush footprint model, and W_s is the stroke width. Since the brush footprint representation is expressed by several 6-order equations, steepest method is applied to find the values that minimize (4). Yet, for the starting point of a trajectory, we initialize (d, γ) to just touch the paper (e.g. $(0, 5^\circ)$), because the cross-section line is just a point.

In addition, the searching range of brush vertical inclination is also limited between 5° and 20° , although our brush footprint model is compatible to larger inclinations. The reason is that the brush is kept vertical, when an artist is writing Chinese calligraphy. This approach would reduce the variation of brush orientation in motions, so the manipulator can be executed with less vibration.

The trajectory searching process is as illustrated in Figure 7. Trajectories are searched along the stroke medial axes (Figure 7(a)). The red shape indicates the brush footprint that is mapping on the stroke. Even the medial axis turns (Figure 7(b)), and the brush footprints also follow the direction of it. This mapping continues, until it reaches to the other termination of the stroke (Figure 7(c)). Then, the discrete path are linearly interpolated to form a complete 5-DOF trajectory.

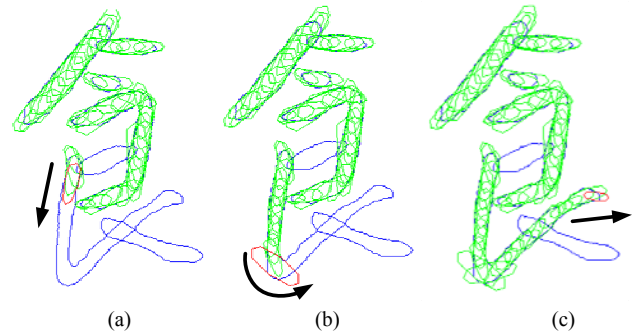


Figure 7. Trajectory searching along the stroke medial axes.

B. Improvement of Trajectory

After the searching, although a trajectory can be obtained for IRAS to execute. However, if only the width is considered, it may superimpose a brush footprint that is outside the stroke boundary as shown in Figure 8(a). In that case, the size of the outlier should be reduced to ensure the executed output is

enclosed in the stroke boundary. As an example, vertex A in the figure is chosen to shrink the brush footprint, because it has the largest distance to the stroke boundary compared to the others. The distance can be expressed to be

$$\Delta D = \|P_i(d, \gamma) - P_S\| \quad (5)$$

where $P_i(d, \gamma)$ is the coordinates of vertex A (i.e. (x_i, y_i)), P_S is the coordinates of the closet point in the stroke boundary and $\|\cdot\|$ is the Euclidean norm. If this distance is minimized by varying the brush positioning parameters, the brush footprint would potentially shrink and just touch the stroke boundary. At the same time the changes in brush pressure level and brush vertical inclination should also be reduced to minimize the vibration created by the manipulator. Therefore, the problem is formulated as

$$\begin{aligned} & \text{minimize} && \omega_1 \Delta D + \omega_2 \Delta I + \omega_3 \Delta B && (6) \\ & \text{subject to} && \Delta I, \Delta B \geq 0 \end{aligned}$$

where ΔD is the distance of vertex A and the closet point in the boundary, ΔI and ΔB are the changes in the brush inclination and applied brush pressure respectively. ω_1 , ω_2 and ω_3 are the coefficients of ΔD , ΔI and ΔB . The resized brush footprint is shown in Figure 8(b). Most of it is overlapped on the stroke, and only small area is not bounded. Sometimes, if the brush footprint cannot be resized to desired size in one time, the shrinking process would continue iteratively for further size reduction.

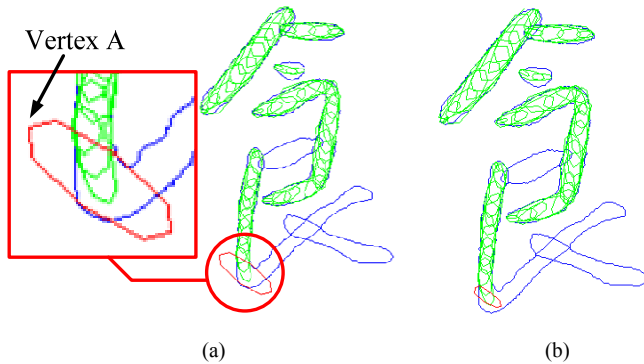


Figure 8. Shrinking the size of the outlying brush footprint: (a) Indication of an outlying brush footprint and (b) the size-reduced brush footprint;

C. Experiments

In this experiment, a Chinese character written by a famous Chinese ancient artist Bada Shanren is used as an example, which is shown in Figure 9(a). The coefficients used in (6) is set to be $\omega_1 = 1$, $\omega_2 = 0.8$ and $\omega_3 = 0.5$. ω_1 is largest to signify the dominant goal of the optimization problem; while ω_2 is greater than ω_3 , since the change of brush pressure level affects less to the system vibration. Figure 9(b) shows the 5-DOF trajectory generated by the improved searching method. The x-y components of the trajectory are discovered to be rugged. However, the rotational axes would compensate the differences, so the center of the brush footprint would move in a smooth path.

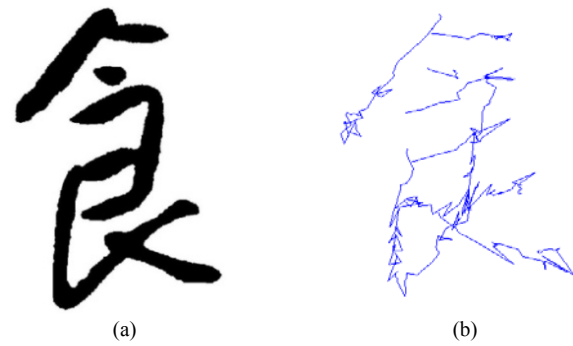


Figure 9. Trajectory searching: (a) The original Chinese character and (b) the trajectory obtained from the improved stroke trajectory searching method

Simulations were carried out, which were displayed in Figure 10(a) and (c). It shows that the trajectory of the preliminary method would generate many regions outside the stroke boundaries, while that of the improved one would ensure the character would similar to the original character. Experiments were also conducted to execute the 5-DOF trajectory using IRAS. Figure 10(b) and (d) are the replicated versions of the character in Figure 9(a) using the preliminary and improved method respectively. The trajectory of the preliminary method has given an expected result with many outlying regions. The largest outlying region is indicated in the red circle. It is different from the simulation result, since the direction of brush motion was changing. For the improved approach, it has a great enhancement in preventing the appearance of outlying regions. Then, it is applied to a passage of calligraphy. The original characters are shown in Figure 11(a), and Figure 11(b) is replicated by IRAS. This calligraphy replication has a satisfied result.

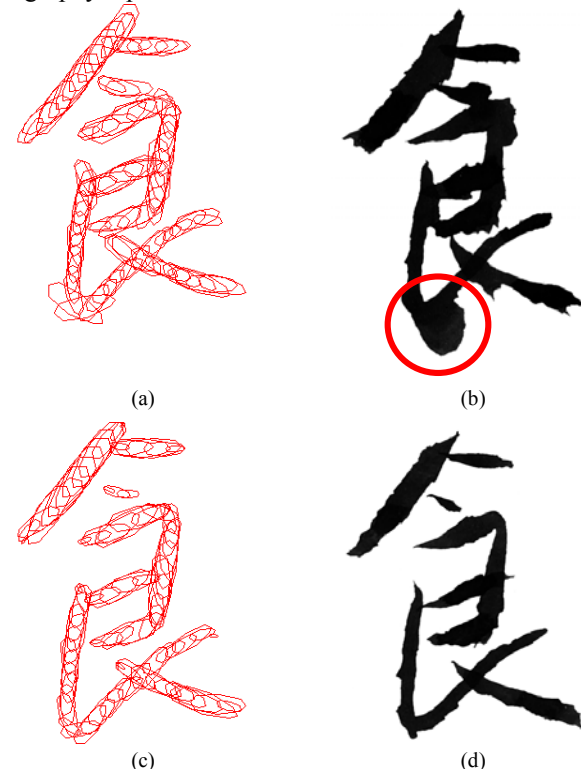
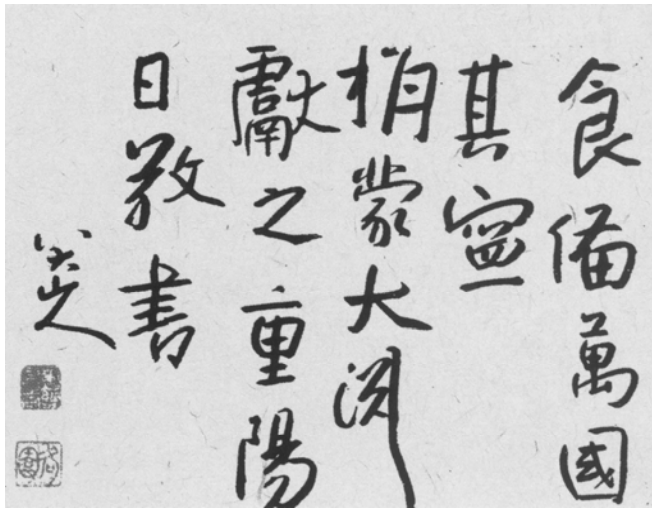
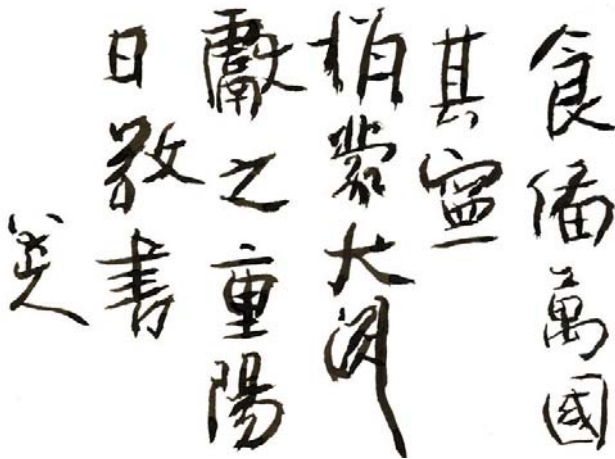


Figure 10. Simulations and results of calligraphy writing: (a)-(b) wide-matching approach and (c)-(d) the improved method.



(a)



(b)

Figure 11. Calligraphy replication: (a) a Chinese calligraphy by Bada Shanren and (b) its replicated version written using IRAS

V. CONCLUSION AND FUTURE WORKS

In this paper, 5-DOF trajectory generation for Chinese calligraphy is investigated, which works with a brush footprint model acquired from experiments. Real brush footprints are extracted experimentally with different brush pressure levels and brush vertical inclinations for the brush model construction. The algorithm searches trajectories by mapping the model with the same widths to the strokes along its center lines. To ensure the brush footprints are surrounded by the stroke boundaries, the trajectories are further modified to reduce the size of them. Results demonstrate that this modification is essential to reduce the outlying regions of the calligraphy. We have also experimentally shown that the proposed trajectory generation would eventually realize robotic Chinese calligraphy. However, the current approach limit the brush moving in longitudinal direction to ensure the brush footprint deforms in a predictable way.

VI. ACKNOWLEDGMENT

This work described in this paper was partially supported by a grant from the Research Grant Council of the Hong Kong Special Administration Region, China (Project No. CUHK 417606) and affiliated with the CUHK MoE-Microsoft Key Laboratory for Human-centric Computing and Interface Technologies.

REFERENCES

- [1] T. Fukuda, J. Taguri, F. Arai, M. Nakashima, D. Tachibana, Y. Hasegawa, "Facial expression of robot face for human-robot mutual communication," Proceedings of International Conference on Robotics and Automation (ICRA '02), vol. 1, pp. 46-51, 2002.
- [2] R. Dance, K. Kosuge, T. Hayashi, Y. Hirata and R. Tobiyama, "Dance Partner Robot - Ms," Proceedings of IEEE/RSJ International Conference on Intelligent Robots and Systems, vol. 4, pp. 3459 - 3464, 2003.
- [3] J. Or and A. Takanishi, "A Biologically Inspired CPG-ZMP Control System for the Real-time Balance of a Single-legged Belly Dancing Robot," Proceedings of IEEE/RSJ International Conference on Intelligent Robots and Systems, vol. 1, pp. 931 - 936, 2004.
- [4] P. McCorduck, "Aaron's Code: Meta-art, Artificial Intelligence and the work of Harold Cohen," W. H. Freeman & Co., New York, New York Copyright 1991.
- [5] L. Pagliarini, and H.H. Lund, "Art, Robots, and Evolution as a Tool for Creativity," Creative Evolutionary Systems, 2001.
- [6] A. Srikaew, M.E. Cambron, S. Northrup, R.A. Peters II, D.M. Wilkes, and K. Kawamura, "Humanoid Drawing Robot," IASTED International Conference on Robotics and Manufacturing, Banff, Canada, July, 1998.
- [7] P. Monaghan, "An art professor uses artificial intelligence to create a computer that draws and paints," The Chronicle of Higher Education, pp. 27-28, May 1997.
- [8] Josh H. M. Lam, K. W. Lo, Y. Yam, "Robot Drawing Techniques for Contoured Surface Using an Automated Sketching Platform," Proceedings of the 3rd Annual IEEE Conference on Automation Science and Engineering, Scottsdale, Arizona, USA, September, 2007.
- [9] Horace H. S. Ip, Helena T. F. Wong, "Calligraphic Character Synthesis using Brush Model," Computer Graphics International 1997 (CGI'97), pp. 13-21, Jun. 1997
- [10] Nelson S. H. Chu and C. L. Tai, "Real-time Painting with an Expressive Virtual Chinese Brush," IEEE Computer Graphics and Applications, vol. 24, issue 5, pp. 76-85, Sept. 2004.
- [11] F. Yao, G. Shao, "Painting brush control techniques in Chinese painting robot," IEEE International Workshop on Robot and Human Interactive Communication, Roman, pp. 462 - 467, 13-15 Aug. 2005.
- [12] N. S. H. Chu, C. L. Tai, "Real-time painting with an expressive virtual Chinese brush," IEEE Computer Graphics and Applications, vol. 24, issue 5, pp. 76 - 85, Sept. 2004.
- [13] X. Mi, J. Xu, M. Tang, J.X. Dong, "The droplet virtual brush for Chinese calligraphic character modeling," Proceedings of the 6th IEEE Workshop on Applications of Computer Vision (WACV 2002), pp. 330 - 334, 3-4 Dec. 2002.
- [14] K. W. Kwok, K. W. Lo, S. M. Wong, Y. Yam, "Evolutionary Replication of Calligraphic Characters By A Robot Drawing Platform Using Experimentally Acquired Brush Footprint," Proceedings of IEEE International Conference on Automation Science and Engineering (CASE 2006), China, pp. 466 - 471, Oct, 2006.
- [15] K. W. Kwok, S. M. Wong, K. W. Lo, Y. Yam, "Genetic Algorithm-Based Brush Stroke Generation for Replication of Chinese Calligraphic Characte," IEEE Congress on Evolutionary Computation (CEC 2006), pp. 1057 - 1064, 2006.
- [16] Josh H. M. Lam, Y. Yam, "A Skeletonization Technique Based on Delaunay Triangulation and Piecewise Bezier Interpolation," Proceedings of the 6th IEEE International Conference on Information, Communications and Signal Processing, Singapore, December, 2007